Title

Hybrid Biological–Chemical Approach Offers Flexibility and Reduces the Carbon Footprint of Biobased Plastics, Rubbers, and Fuels

Journal

ACS Sustainable Chemistry & Engineering, 6(11)

ISSN

2168-0485

Authors

Wu, Lipeng
Gokhale, Amit
Goulas, Konstantinos A
et al.

Publication Date

2018-11-05

DOI

10.1021/acssuschemeng.8b03158

Peer reviewed

A hybrid biological-chemical approach offers flexibility and reduces the carbon footprint of bio-based plastics, rubbers, and fuels

Lipeng Wu[1,2,3*], Amit Gokhale[1,4*], Konstantinos A. Goulas[1,2,5], John E. Myers[6], F. Dean Toste[1,2], Corinne D. Scown[1,7,8*]

[1] Energy Biosciences Institute, Berkeley, CA 94720

[2] College of Chemistry, University of California, Berkeley, Berkeley, CA 94720

[3] State Key Laboratory for Oxo Synthesis and Selective Oxidation, Suzhou Research Institute of Lanzhou Institute of Chemical Physics, CAS, Lanzhou 730000 (P. R. China)

[4] BASF Corporation, 33 Wood Avenue South, Iselin, NJ 08830.

[5] Oregon State University, School of Chemical, Biological and Environmental Engineering, Corvallis, OR 97331

[6] University of Wyoming, Chemical and Petroleum Engineering, Laramie, WY 82071

[7] Joint BioEnergy Institute, Emeryville, CA.

[8] Energy Analysis and Environmental Impacts Division, Lawrence Berkeley National Laboratory, Berkeley, CA 94720

*Corresponding authors: E-mail: lipengwu@licp.cas, amit.gokhale@basf.com, cdscown@lbl.gov

Keywords: Biofuels, bioproducts, catalysis, butadiene, life-cycle assessment, greenhouse gases

Abstract

A critical challenge for the bioenergy research community has been producing drop-in hydrocarbon fuels and chemicals at yields sufficient to compete with their petroleum-derived counterparts. Biological production of highly reduced compounds poses fundamental challenges. Conversely, glucose, xylose, and sucrose can be fermented to ethanol at near-theoretical yields. Just as olefin crackers are often considered a gateway for petrochemical complexes that produce an array of downstream products, catalytic ethanol upgrading can potentially enable an entire biorefining complex able to produce renewable, low-carbon fuels and chemicals. By doping the Ta_2O_5/SiO_2 catalyst with different transition metals, we show that Ostromyslensky catalysts can be utilized for direct conversion of ethanol to varying ratios of 1,3-BD, dietheylether (DEE), and ethylene. These results are integrated into the first comprehensive analysis of ethanol conversion to 1,3-BD, DEE, and ethylene that incorporates empirical data with chemical process modeling and life-cycle GHG assessment. We find that the suite of products can replace conventional rubber, plastics, and diesel, achieving as much as a 150% reduction in GHG-intensity relative to fossil pathways (net carbon sequestration). Selecting the route with greatest ethylene and DEE output can maximize total potential emission reductions.

Introduction

Over time, petrochemical refineries have optimized their processes to convert each barrel of crude oil to a slate of products to maximize their profitability. Recent fluctuations notwithstanding, the rise in crude oil prices over the last five decades, paired with policies aimed at reducing reliance on fossil energy, has made renewable fuels and chemicals an attractive proposition. Ethanol produced from sugarcane and starch, as well as some of the renewably-sourced chemicals such as diols and diacids, have approached cost parity with their fossil-derived counterparts.[1–4] Bio-based ethanol has been used as a fuel for internal combustion engines as early as the 1800's, and re-emerged on the market as a useful oxygenate and octane booster for spark-ignited engines in the 1990's.[5] Depending on the feedstock, ethanol can also dramatically reduce transportation-related greenhouse gas (GHG) emissions, but its market penetration is limited in part by the blend wall.[6] Although recent studies have explored the possibility of biologically producing molecules that better mimic the properties of conventional hydrocarbons, yields must be improved before these pathways can be commercialized.[7,8]

In the competitive petrochemicals market, high yields are essential, and ethanol offers an attractive starting point, since fermentation yields from sugars such as glucose, xylose, and sucrose are close to theoretical limits.[9] Just as olefin crackers are often considered a gateway for petrochemical complexes that produce an array of downstream products, catalytic ethanol upgrading has the potential to enable an entire biorefining complex able to produce renewable, low-carbon fuels and chemicals.[10] In this paper, we investigate this possibility by studying the conversion of ethanol to 1,3-butadiene (1,3-BD), ethylene, and diethyl ether (DEE). Products such as 1,3-BD and ethylene play an important role in the polymers market while DEE is a useful solvent and can serve as a diesel substitute.[11]

Recently, there has been renewed interest in the Lebedev process, which involves an one-step conversion of ethanol into 1,3-BD.[12–14] This process utilizes MgO/SiO_2-based catalysts and has been shown to give single-pass yields of ~70%, but considerably lower yields at industrially-relevant ethanol partial pressures.[15–19,19] Another process of interest was developed by Ivan Ostromyslensky, which involves two distinct steps, i.e. dehydrogenation of ethanol into acetaldehyde over a dehydrogenation catalyst and subsequent conversion of mixtures of acetaldehyde and ethanol into 1,3-BD over Ta_2O_5/SiO_2 catalysts.[20,21] Since the dehydrogenation step is endothermic and equilibrium-limited at lower temperatures (Figure S1), an oxidative dehydrogenation is often preferred. Such a process oxidizes hydrogen, which is otherwise a valuable byproduct of the process. Because of this, coupling the dehydrogenation step with C-C bond formation step is very advantageous, as it removes the equilibrium limitation (Figure S1).

To understand the potential for direct conversion of ethanol to 1,3-BD, DEE, and ethylene mixtures using Ostromyslensky's pathway and evaluate the industrial relevance and value of these mixtures, we combine an experimental investigation with chemical process modeling and life-cycle GHG assessment. We hypothesize that, by doping the Ostromyslensky Ta_2O_5/SiO_2 catalysts with suitable transition metals, we can achieve direct conversion of ethanol to 1,3-BD, DEE, and ethylene (with a range of product ratios) over a single catalyst. To understand how these products compare on a GHG basis, we then conduct the first comprehensive GHG assessment of ethanol conversion to these bioproducts by linking chemical process modeling and life-cycle assessment (LCA). This approach allows us to explore the yield variations, impacts of downstream processing/separations on the mass and energy balance, and potential impact on net GHG emissions for the catalytic conversion of ethanol to varying mixtures of 1,3-BD, ethylene, and DEE for the production of rubber, plastics, and diesel blendstock, respectively.

Methodology

Selecting Transition Metal Catalysts

Several mechanistic investigations have demonstrated that the ethanol to 1,3-BD reaction proceeds via 5 key steps, shown in scheme 1: a) dehydrogenation of ethanol to acetaldehyde, b) aldol condensation of acetaldehyde to 3-hydroxybutanal, c) dehydration of 3-hydroxybutanal to crotonaldehyde, d.) reduction of crotonaldehyde to crotyl alcohol with ethanol and e.) dehydration of crotyl alcohol to 1,3-BD.[5,22–24]

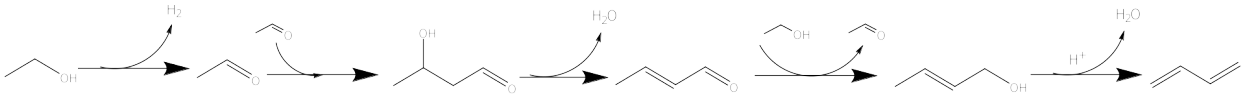

Scheme 1: Reaction Pathway for the Production of 1,3-BD from Ethanol.

While the aldol condensation step takes place over basic or acid sites, dehydrogenation may occurs predominately over redox site.[25] Acid sites are also required for the dehydration steps. A good E2B catalyst therefore needs to have a combination of active acidic, basic and redox sites and their number, strength, and proximity are all important considerations.[25] MgO/SiO_2 has long been the chosen catalyst for the reaction and some of our recent studies[13] and research from Weckhuysen, Bruijnincx[26], and Jones[27,28], have shown that when doped with suitable metals such as Cu, Ag, or Au, it is possible to tune the selectivity for 1,3-BD. Taking inspiration from these studies we sought to study the Ta_2O_5/SiO_2 catalysts traditionally used in Ostromyslensky two-step process. We developed several new catalysts by doping different transition metals and metal oxides on the Ta_2O_5/SiO_2 catalysts and chose to study the variations in products obtained from the reaction under industrially relevant reaction conditions.[28] Given the value of side products previously considered undesirable, we also chose to test a range of doped Ta_2O_5/SiO_2 catalysts capable of producing a variety of product distributions including 1,3-BD, ethylene, and DEE.[29]

Jones and colleagues have shown that dehydration of ethanol to ethylene is favored on SiO_2 at 375 ℃. At 300 ℃, we find that acetaldehyde is the major product though the conversion was quite low (Table 1, Entry 2). Crystalline β-Ta_2O_5 favors the formation of acetaldehyde as well as DEE (Table 1, Entry 3). Doping 20% Ta on silica results in a catalyst that is active but such a catalyst rich in acid sites primarily produces the products of dehydration, i.e. ethylene and diethyl ether (Table 1, Entry 4). In order to increase selectivity to acetaldehyde, we need to introduce a dehydrogenation active site. While Pd increased the dehydrogenation rate, the decarbonylation of the resulting acetaldehyde was also rapid, resulting in high methane selectivity (Table 1, Entry 5). Modest improvements were achieved by addition of Ni, Au[13] and Pd/Cu alloys[30] (Table 1, Entries 6-7). Ag[31] (Table 1, Entry 8) and Cu[26] (Table 1, Entry 9), consistent with literature findings, significantly improved the butadiene yields. However, the highest butadiene yield was achieved by the

addition of Zn[32,33] to the Ta_2O_5/SiO_2 (Table 1, Entry 11). With ZnO with either SiO_2 or Ta_2O_5 gave mainly acetaldehyde as products. Supported[34] and unsupported[35] Zn oxides have been reported to catalyze alcohol dehydrogenation reactions by means of the lattice oxygen atoms or defects and vacancies in the structure and our results are consistent with this observation.

Table 1: Metal Dopant Effects on Ethanol Conversion and Product Distribution (WHSV* 0.4 h^{-1}, 573 K, TOS = 180 min)**

Entry	Catalyst	Ethanol Conversion (%)[a]	Selectivities (C mol%)[a]				
			Butadiene	Acetaldehyde	Ethylene	Diethyl Ether	Others[b]
1	-	1.9	-	100	-	-	-
2	SiO_2	4	-	97.4	2.6	-	-
3	Ta_2O_5	2.4	-	79.4	-	20.5	-
4	$20\%Ta_2O_5/SiO_2$	28.6	1.5	3.4	32.8	62.2	-
5	$2\%Pd@20\%Ta_2O_5/SiO_2$	49.4	-	4.3	-	-	-[c]
6	$2\%Ni@20\%Ta_2O_5/SiO_2$	22.0	17.0	27.7	11.4	31.4	12.5
7	$2\%Au@20\%Ta_2O_5/SiO_2$	38.3	6.6	6.9	28.5	54.3	3.7
8	$2\%Ag@20\%Ta_2O_5/SiO_2$	39.1	44.0	16.1	19.2	16.9	3.8
9	$2\%Cu@20\%Ta_2O_5/SiO_2$	31.8	45.4	22.0	5.5	4.6	22.5
10	$2\%Pd/Cu@20\%Ta_2O_5/SiO_2$	32.1	12.3	20.6	16.1	26.7	24.3
11[d]	$2\%Zn@20\%Ta_2O_5/SiO_2$	34.7	60.2	18.4	7.2	7.6	6.6
12[d,e]	$2\%Zn@20\%Ta_2O_5/SiO_2$	39.5	50.9	9.0	26.9	2.6	10.6
13[d]	$2\%Zn@SiO_2$	13.3	6.5	81.4	1.9	1.3	8.9
14[d]	$2\%Zn@Ta_2O_5$	12.0	-	87.5	3.8	-	8.7

a. Conversion and selectivities are based on the carbon number, *b*. other chemical contains butenes, crotonaldehyde, 1-butanol, propane and methane, *c*. methane 87.9%, ethane 4.6%. *d*. ZnO were used as Zn source. e. reaction performed at 648 K. * WHSV = Weight Hourly Space Velocity (Mass Flow/Catalyst Mass)** TOS = Time on Stream

Selecting Products of Interest

The results shown in Table 1 indicate that different dopants facilitate production of varying fractions of five products: 1,3-BD, acetaldehyde, butenes, ethylene, and DEE (although only $2\%Cu@20\%Ta_2O5/SiO_2$ resulted in selectivity for butenes greater than a few percent). Of those potential products, ethylene has by far the largest market, at approximately 140 million tonnes per year,[10] sixty percent of which goes towards satisfying global polyethylene demand. Ethylene is also used for the production of ethylene glycol which finds applications in polyester fibers, polyethylene terephthalate (PET) resins, antifreeze, ethyoxylates, glycol ethers, and ethanolamines[36]. Relative to ethylene, 1,3-BD, DEE, and acetaldehyde have much smaller markets at about 14, 12, and 4 million tonnes/year respectively. More than half of 1,3-BD is used in the production of car tires as styrene-butadiene rubber (SBR) and polybutadiene.[37] Other polymers made from 1,3-BD include acrylonitrile-butadiene-styrene (ABS), styrene-butadiene

latex, and chloroprene rubber, several of which are also used in the automotive industry.[38,39] DEE is also used in the automotive sector as engine starting fluid,[40] but if produced in sufficient volumes, its high cetane number (>125) could make DEE an attractive blendstock for conventional diesel, biodiesel, or renewable diesel fuel.[11,41]

From the supply perspective, DEE and 1,3-BD production are closely tied to ethylene production, with almost 95% of current 1,3-BD produced as a byproduct from ethylene crackers. Ethylene can also undergo vapor-phase hydration to produce ethanol, which is in turn the primary feedstock for DEE production. 1,3-BD prices closely tracked ethylene prices for decades, but in 2011-2012, 1,3-BD prices spiked far above those of ethylene, from less than $1000 USD/tonne to nearly $5000/tonne at its peak.[42] In response to this price spike, at least 13 energy-intensive on-purpose butadiene facilities were planned or constructed in 2012 to produce butadiene from *n*-butane or *n*-butene, shortly before the price collapsed in 2013.[43] A process for converting ethanol to 1,3-BD would serve as a viable renewable alternative to the Oxo-D™ or Houndry Catadiene process in the event of another more sustained price spike. Co-producing ethylene and DEE can help meet enormous demand for polymers and diesel fuel, respectively. In fact, a high-level screening of potential ethanol-based products on the basis of economic constraints, environmental impacts, and health and safety risks indicated that 1,3-BD and DEE were the two most favorable products of the ten options evaluated.[44] Moreover, an approach that allows for varying product ratios through different catalysts or reaction conditions could offer flexibility in responding to the shifting balance between demand and supply for platform chemicals. For these reasons, we chose to focus on 1,3-BD, DEE, and ethylene as our products of interest.

Developing Biorefinery Configurations

Based on the selectivity for 1,3-BD, DEE, and ethylene, we chose four representative sets of results and modeled the corresponding biorefinery configurations starting with ethanol as a feedstock to produce 1,3-BD, ethylene, and/or DEE at purities required to meet industry specifications (Table 2 references the original tables in the main text and SI where each set of empirical results were reported). We simulated and analyzed the mass and energy flows for each 400,000 ton/year biorefinery in Aspen Plus. Because we are only modeling these biorefinery configurations to determine mass and energy balances, the assumed scale impacts our results less than would be the case in a cost-focused study. A commercial facility may ultimately have a smaller capacity (100,000-200,000 tons ethanol intake/year). For example, a 100,000 ton/year plant would require a catalyst volume of approximately 50 m^3, which could be accommodated in 3 shell-and-tube reactors. Further optimization of the catalyst in scale-up studies could be achieved to reduce the reactor size required.

Our model is based on an intake of anhydrous ethanol, but it is worth noting that the presence of water does not deactivate the catalyst and it may be advantageous to accept hydrous ethanol in some cases. A molecular sieve system alone can require on the order of 0.1-1% of the energy content of ethanol output to dehydrate the ethanol product beyond the 95.63% ethanol / 4.37% water azeotrope to reach motor fuel standards. Avoiding this step could save energy and capital costs at ethanol production facilities. We do not assume these biorefineries are co-located with cellulosic or corn ethanol production facilities, so energy needs not satisfied by the combustion of minor products onsite must be met by electricity imported from the grid and imported natural gas for thermal energy. We do assume that the biorefineries are located in close proximity to facilities able to use excess hydrogen, and that any excess hydrogen offsets the need for hydrogen production via steam-reforming of natural gas. This choice is based on the fact that ethanol is relatively easy to transport in trucks, marine tankers, and tanker rail cars, whereas gaseous products are more challenging to transport and selecting conversion facilities near markets for gaseous products such as hydrogen and ethylene is likely to be an optimal strategy.

Table 2 Cases Selected for Biorefinery Models (Selectivity based on TOS = 180 min)

Case	Corresponding Result	Catalyst	Selectivity (C mol %)			
			1,3-Butadiene	Ethylene	Diethyl Ether	Other Products Recycled and/or Combusted On-Site
A	Table 1 Entry 4	20%Ta2O5/SiO2	N/A	32.8	62.2	3.4
B	Table 1 Entry 12	2%Zn@20%Ta2O5/SiO2	50.9	26.9	N/A	22.2
C	Table S2 Entry 8	2%Zn@50%Ta2O5/SiO2	44.4	13.1	19.7	22.8
D	Table 1 Entry 11	2%Zn@20%Ta2O5/SiO2	60.2	7.2	7.6	25.0

Life-Cycle Greenhouse Gas Inventory

To complete the life-cycle GHG modeling for this study, we developed a variation on the standard hybrid LCA approach, which combines process-based modeling for key components of the supply chain with input-output analysis to account for indirect contributors to GHG emissions, documented in three prior articles.[45–47] The outputs from the AspenPlus process models described in the previous section are linked with our hybrid life-cycle assessment (LCA) model by importing values for specified inlet and outlet streams (ethanol intake and 1,3-BD output, for example) and assigning those values to the appropriate parameters in the LCA. A set of simple functions are used to convert these values into direct inputs and outputs, and

generate other important parameters such as transportation distances for biomass, ethanol, and end products. The mass and energy balances for the baseline fossil-based routes are derived from literature (sources listed in Table S4).

The key difference in our approach for the input-output section of the model is that, rather than relying on the sector-oriented Economic Input-Output Life-Cycle Assessment (EIO-LCA) model, our model uses a specialized produced and service-oriented direct requirements matrix based on physical units (typically mass or energy, depending on the product). The matrix includes all products and services expected to contribute appreciably to life-cycle GHG emissions, further detailed in the Supporting Information. The impact vector, which consists of direct GHG emissions (in CO_{2e}) per physical unit output for each product or service, is multiplied by the result to yield the full life-cycle emissions. The equation used to calculate life-cycle emissions is shown in Equation 1. There are, of course, many data sources and methodological choices embedded in the impact vectors and input-output table. Table S4 provides direct GHG emission factors for every production process required directly or indirectly in the bio-based and conventional production routes, allocation methods utilized to calculate these factors (where applicable), other key assumptions used in the analysis, and specific data sources.

Equation 1: Input-Output LCA Model Structure

$$b = R_p\left(I - A_p\right)^{-1} y_p$$

Where b=¿ total life-cycle GHG emissions, I=¿ identity matrix, A_p=¿ input-output matrix in physical units, y_p=¿ final demand vector in physical units, and R_p=¿ diagonalized GHG impact vector based on physical units

Results and Discussion

Variations in Product Distributions

A mechanistic understanding of various elementary steps on the catalytic surface allowed us to control the product distribution. For example, we tuned the Zn and Ta content of the catalysts in order to selectively target products of interest (Figure 1 and Table S2). We found that increasing Zn content from 0.4 to 4 wt% led to an increase in ethanol conversion and butadiene selectivity while decreasing the selectivity to ethylene and diethyl ether (Figure 1 left side, Table S2, Entries 1-4). This suggests that Zn introduces redox and basic site and/or blocks some of the acid sites on Ta_2O_5/SiO_2, which are known to catalyze dehydration chemistry. Interestingly, increasing Zn content to 8% reduced butadiene selectivity significantly, giving instead oligomers and reduced products, such as butanol. This is in agreement with

studies by Kyriienko[32] and Cavani[22] and we hypothesize that drastic reduction of acid sites can impact the dehydration of crotyl alcohol to 1,3-BD. At the same time, Zn may also increase hydrogenation activity causing conversion of crotonaldehyde and crotyl alcohol to butyraldehyde and butanol (Table S2, Entry 5). The increased hydrogenation-dehydrogenation catalysis by Zn could also be responsible for improved selectivity for aldol condensations to longer oligomers. Consistent with this interpretation, we found that increasing the Ta_2O_5 content of the catalyst from 5% to 20% Ta_2O_5, increased the butadiene selectivity (Figure 1 right side, Table S2, Entries 6-8). Increasing Ta_2O_5 to 50 wt% created more acidic sites which led to more ethylene and diethyl ether (Table S2, Entry 8). This mechanism guided the development of catalysts, allowing us to tune the relative proportion of Ta and Zn to obtain the desired product composition.

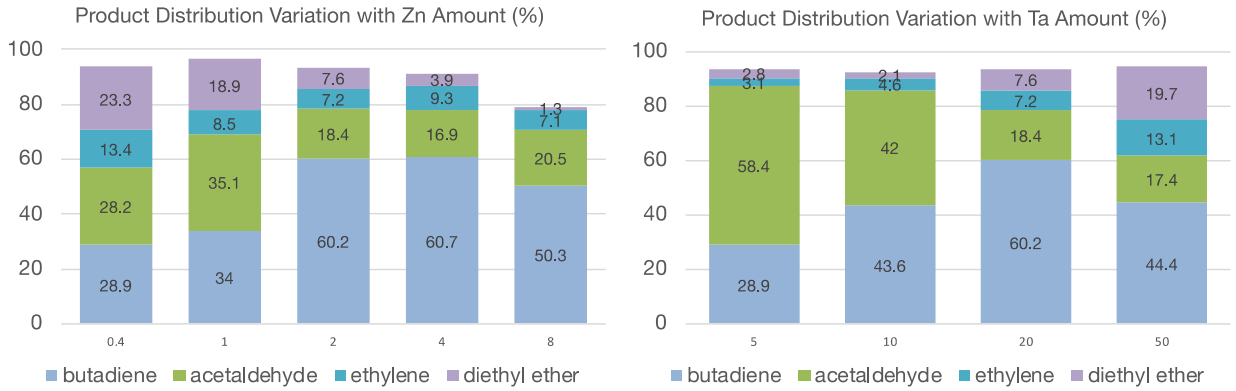

Figure 1: Ratio of Selected Products by Catalyst Composition (see SI for Detailed Products Distribution)

In addition to the dopant concentrations, the partial pressure and temperature also have a strong effect on the product distribution (Table S3). We found that increasing the ethanol partial pressure increased ethanol conversion and favored selectivity towards ethylene and DEE at the expense of butadiene (Table S3, Entries 1-3). Increased ethanol partial pressure may promote bimolecular dehydration, leading to improved selectivity towards DEE.

A probe into temperature effects showed that while acetaldehyde was the major product at temperatures below 573 K (Table S3, Entry 5), at higher temperatures, ethylene and butadiene production were favored (Table S3, Entries 7-9). Mechanistically, both these reactions involve a unimolecular dehydration step. This suggests that higher temperatures favor unimolecular dehydration, consistent with the thermodynamics (Figure S1). Further temperature increases did not result in increased conversion, but in increased dehydration of ethanol to ethylene.

In order to better understand the relative rates of various reactions, a selectivity/conversion plot is quite useful. Based on , we conclude that the butadiene is produced as a secondary product from acetaldehyde. Acetaldehyde selectivity is high initially and drops as butadiene selectivity increases from zero. Acid chemistry product selectivity does not change appreciably as a function of conversion. However, the ratio of DEE to ethylene in the products increases as the pressure of ethanol increases, reflecting the fact that the formation of DEE requires the presence of two ethanol molecules, as opposed to ethylene formation [48].

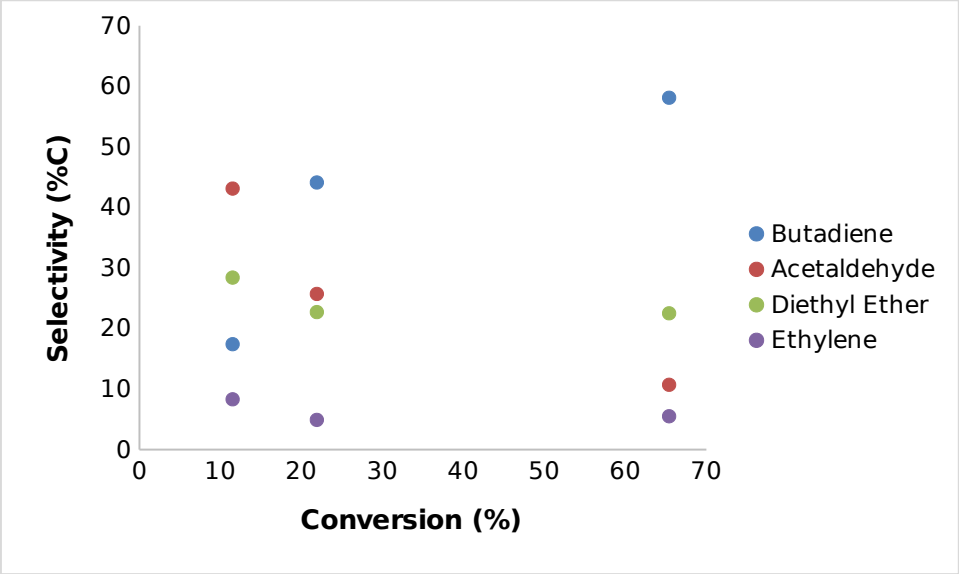

Figure 2: Effects of Percent Conversion on Selectivity

Developing Biorefinery Configurations

Figure 3 shows the simplified process flow diagrams for each biorefinery corresponding to the results in Table 2, labeled A, B, C, and D. Separations processes present the most significant challenges for these configurations, as the compounds present in the biorefineries form four different azeotropes: acetaldehyde (76%) and DEE (24%), ethanol (95.5%) and water (4.5%), DEE (98.7%) and water (1.3%), and butadiene (94.8%) and acetaldehyde (5.2%). In each case, conversion of ethanol to products occurs in a single reactor and the remaining processes are devoted to product recovery. Unconverted ethanol and acetaldehyde are recycled, and water is sent to an offsite wastewater treatment facility. Ethylene is recovered at or above 99.7% purity in all cases, butadiene is recovered at purities above 98.2%, and DEE is recovered at greater than 97.3% purity. Exported hydrogen is greater than 95% pure. In Case B, pressure swing adsorption is required to recover the hydrogen-rich stream from the primarily hydrogen-ethylene mixture. Small butane-rich streams are combusted onsite, as is a small ethylene stream that could not be purified to reach the 99.7% purity threshold. Each model is based on the best available results demonstrated at lab scale. Increasing the

conversion rate in subsequent research will reduce the volume of recycle streams required, which will reduce the reactor size needed and improve the likelihood of cost-competitiveness. The process models outlined here account for the energy impacts of recycle streams (and associated impacts on separations systems), and if conversion can be improved, this will also ultimately reduce on-site energy demand.

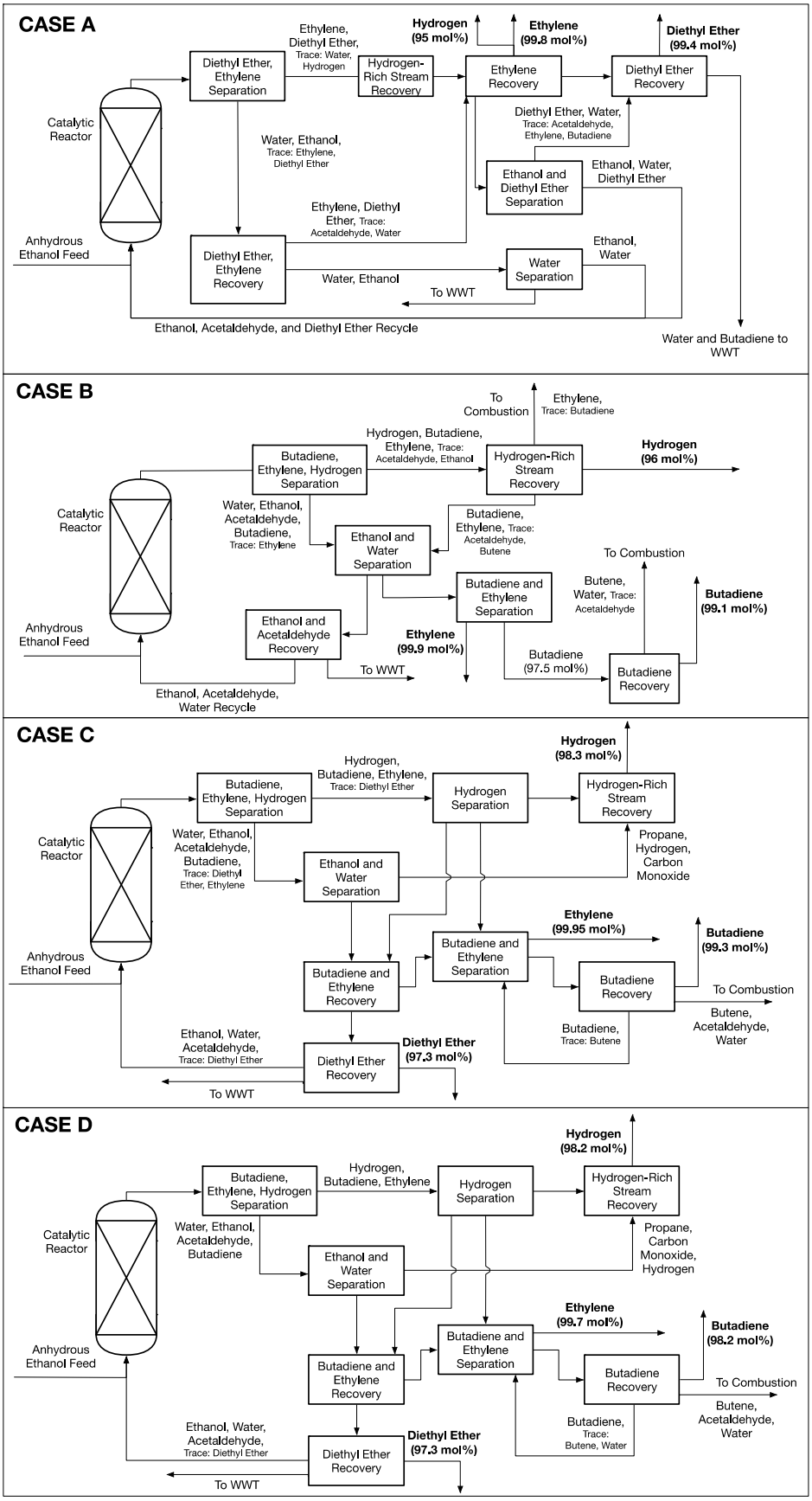
CASE A
Ethylene, Diethyl Ether, Trace: Water, Hydrogen
Hydrogen (95 mol%)
Ethylene (99.8 mol%)
Diethyl Ether (99.4 mol%)
Diethyl Ether, Ethylene Separation
Hydrogen-Rich Stream Recovery
Ethylene Recovery
Diethyl Ether Recovery
Catalytic Reactor
Diethyl Ether, Water, Trace: Acetaldehyde, Ethylene, Butadiene
Water, Ethanol, Trace: Ethylene, Diethyl Ether
Ethanol and Diethyl Ether Separation
Ethanol, Water, Diethyl Ether
Ethylene, Diethyl Ether, Trace: Acetaldehyde, Water
Anhydrous Ethanol Feed
Diethyl Ether, Ethylene Recovery
Water Separation
Ethanol, Water
Water, Ethanol
To WWT
Ethanol, Acetaldehyde, and Diethyl Ether Recycle
Water and Butadiene to WWT
CASE B
To Combustion
Ethylene, Trace: Butadiene
Hydrogen, Butadiene, Ethylene, Trace: Acetaldehyde, Ethanol
Butadiene, Ethylene, Hydrogen Separation
Hydrogen-Rich Stream Recovery
Hydrogen (96 mol%)
Catalytic Reactor
Water, Ethanol, Acetaldehyde, Butadiene, Trace: Ethylene
Butadiene, Ethylene, Trace: Acetaldehyde, Butene
Ethanol and Water Separation
To Combustion
Butene, Water, Trace: Acetaldehyde
Butadiene and Ethylene Separation
Butadiene (99.1 mol%)
Anhydrous Ethanol Feed
Ethanol and Acetaldehyde Recovery
Ethylene (99.9 mol%)
Butadiene (97.5 mol%)
To WWT
Butadiene Recovery
Ethanol, Acetaldehyde, Water Recycle
CASE C
Hydrogen (98.3 mol%)
Hydrogen, Butadiene, Ethylene, Trace: Diethyl Ether
Butadiene, Ethylene, Hydrogen Separation
Hydrogen Separation
Hydrogen-Rich Stream Recovery
Catalytic Reactor
Water, Ethanol, Acetaldehyde, Butadiene, Trace: Diethyl Ether, Ethylene
Propane, Hydrogen, Carbon Monoxide
Ethanol and Water Separation
Ethylene (99.95 mol%)
Butadiene (99.3 mol%)
Anhydrous Ethanol Feed
Butadiene and Ethylene Separation
Butadiene and Ethylene Recovery
Butadiene Recovery
To Combustion
Butene, Acetaldehyde, Water
Butadiene, Trace: Butene
Ethanol, Water, Acetaldehyde, Trace: Diethyl Ether
Diethyl Ether (97.3 mol%)
Diethyl Ether Recovery
To WWT
CASE D
Hydrogen (98.2 mol%)
Butadiene, Ethylene, Hydrogen Separation
Hydrogen, Butadiene, Ethylene
Hydrogen Separation
Hydrogen-Rich Stream Recovery
Catalytic Reactor
Water, Ethanol, Acetaldehyde, Butadiene
Propane, Carbon Monoxide, Hydrogen
Ethanol and Water Separation
Ethylene (99.7 mol%)
Butadiene (98.2 mol%)
Anhydrous Ethanol Feed
Butadiene and Ethylene Separation
Butadiene and Ethylene Recovery
Butadiene Recovery
To Combustion
Butene, Acetaldehyde, Water
Butadiene, Trace: Butene, Water
Ethanol, Water, Acetaldehyde, Trace: Diethyl Ether
Diethyl Ether (97.3 mol%)
Diethyl Ether Recovery
To WWT

387

Figure 3: Simplified Process Flow Diagrams for Cases A-D

The resulting major product yields are shown in Figure 4 per kg of ethanol input. Case A maximizes mass output and net heating value of products per unit ethanol input, yielding 0.38 kg ethylene and 0.28 DEE per kg ethanol (1.1 MJ in products per MJ ethanol input HHV). Note that Case A is not net energy-positive, of course, because of natural gas and electricity inputs required. Case B yields 0.45 kg 1,3-BD and 0.040 kg ethylene per kg ethanol (0.79 MJ HHV in products per MJ ethanol input HHV). Case C yields 0.43 kg 1,3-BD, 0.075 kg ethylene, and 0.098 kg DEE per kg ethanol (0.97 MJ HHV in products per MJ ethanol input HHV). Case D yields 0.51 kg 1,3-BD, 0.043 kg ethylene, and 0.010 kg DEE per kg ethanol (0.91 MJ HHV in products per MJ ethanol input HHV). Hydrogen yields are generally lower: Case A yields 0.00053 kg H_2 per kg ethanol, Case B yields 0.017 kg H_2 per kg ethanol, Case C yields 0.016 kg H_2 per kg ethanol, and Case D yields the most at 0.019 kg H_2 per kg ethanol. These masses are based on stoichiometry, combined with the downstream separations required to produce a sufficiently pure H_2 stream for export.

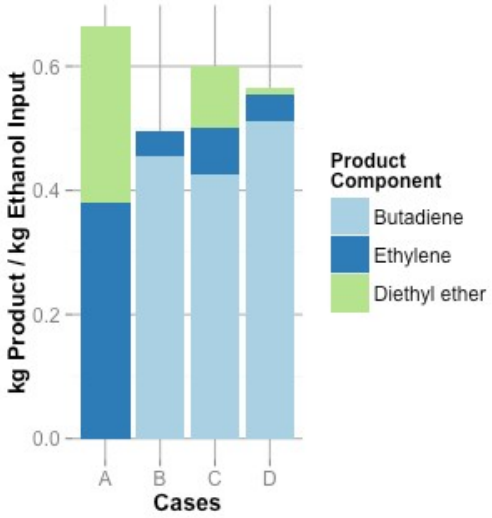

Figure 4: Breakdown of Products by Mass

Life-Cycle Greenhouse Gas Assessment

Using the calculated energy and material balances for each biorefinery configuration, product yields, and a set of potential corn grain, cellulosic, and sugarcane ethanol sources, we conducted a detailed cradle-to-grave life-cycle GHG assessment for each of the four cases described above. Our analysis of 1,3-BD and ethylene is based on their most significant applications: rubber and plastics production, respectively. DEE is modeled as a potential diesel blendstock. We began our analysis by calculating the direct carbon flows, from feedstock, to hydrolysate sugars, through ethanol,

and finally to end products. The flows of carbon atoms for the conversion of corn stover-derived ethanol are shown in Figure 5. Our model is based on the National Renewable Laboratory (NREL) dilute acid corn stover-to-ethanol biorefinery configuration *nth* plant performance.[9,49] In Case A, ethylene and DEE make up the majority of the products, whereas 1,3-BD is the major product in Cases B, C, and D.

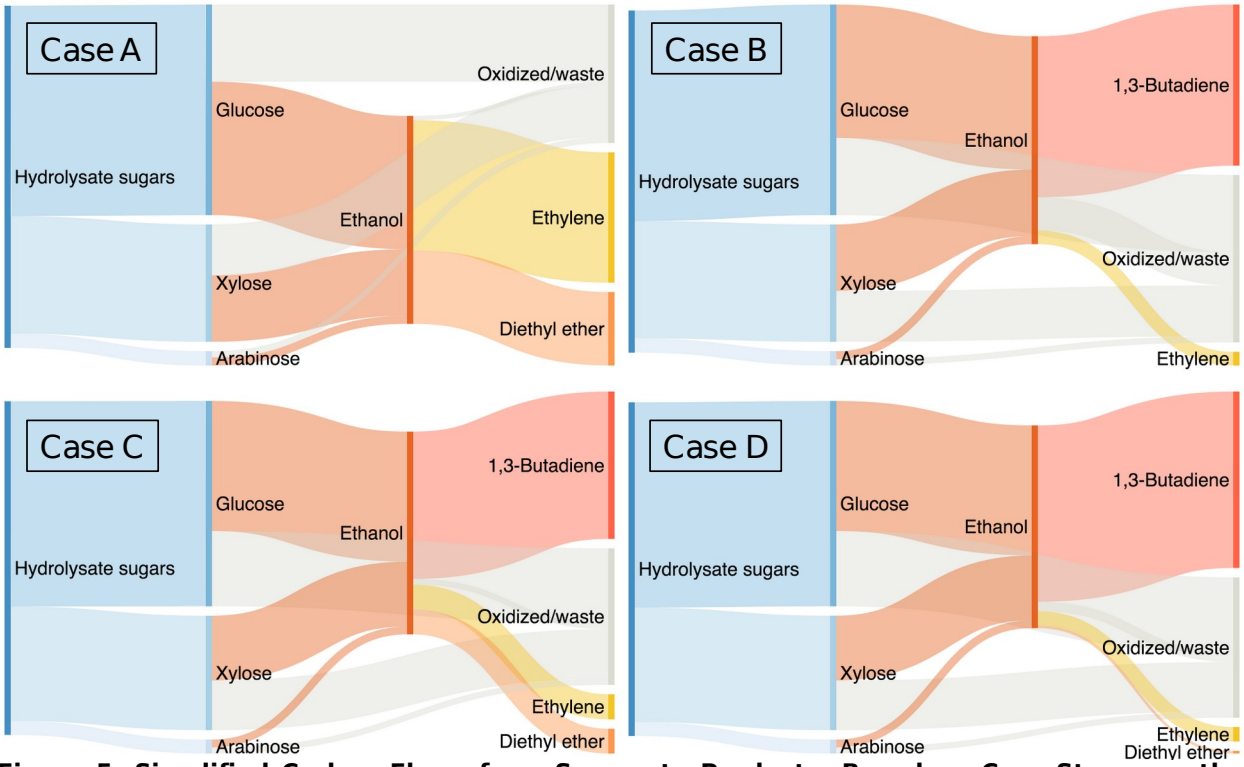

Figure 5: Simplified Carbon Flows from Sugars to Products, Based on Corn Stover as the Feedstock

Figure 6 shows the life-cycle GHG results for each case, using three different feedstocks for the production of ethanol: corn grain, sugarcane, and corn stover. We also modeled the net GHG footprint of fossil-derived products in the ratios produced by Cases A-D, as a basis for comparison. This allows us to avoid selecting inherently imperfect allocation methods, which are a topic of intense debate in the life-cycle assessment community.[50–53] Results are reported on a per-kg basis for the total mix of products. This means results should not be compared across individual cases on a per-kg basis, but rather compared in terms of the percent reduction in GHG emissions achieved by each case relative to the corresponding conventional fossil cases. In the case of DEE, we used the GHG footprint of diesel fuel production, since we assume our DEE product would be used as a diesel blendstock. For each of the conventional products used for comparison (diesel fuel, ethylene, and 1,3-BD), there are embedded allocation methods used to allocate refinery/facility

emissions to those individual products. In all cases, energy content-based allocation was used, and further details are provided in Table S4.

The sensitivity bars shown in Figure 6 represent the impacts of variations in the transportation distances for shipping U.S.-produced ethanol between biorefineries and final conversion facilities (low: 197 km, average: 1586 km, high: 1696) and the offset credits assigned for electricity exports from cellulosic ethanol facilities (low: 100% renewables, average: TRE NERC region mix, high: SPP NERC region mix). The transportation distances for ethanol were calculated using a geographic information systems (GIS) tool (QGIS) and rail network data, with the average distance representing the distance between facilities in Iowa and Texas.

In each case, we account for the fraction of carbon atoms sequestered in landfills or other long-term stable storage (asphalt, for example), and the fraction combusted or otherwise oxidized. Approximately 44% of 1,3-BD is ultimately combusted in the U.S., all DEE will be combusted (assuming it is used as a diesel blendstock), and 7% of ethylene is combusted based on typical plastic incineration rates in the U.S.[54] Our results for the fossil pathways to non-fuel products are similar to existing studies; for example, low density polyethylene (LDPE) resin is estimated to have a life-cycle GHG footprint of 1.9 kg CO2e/kg resin.[55]

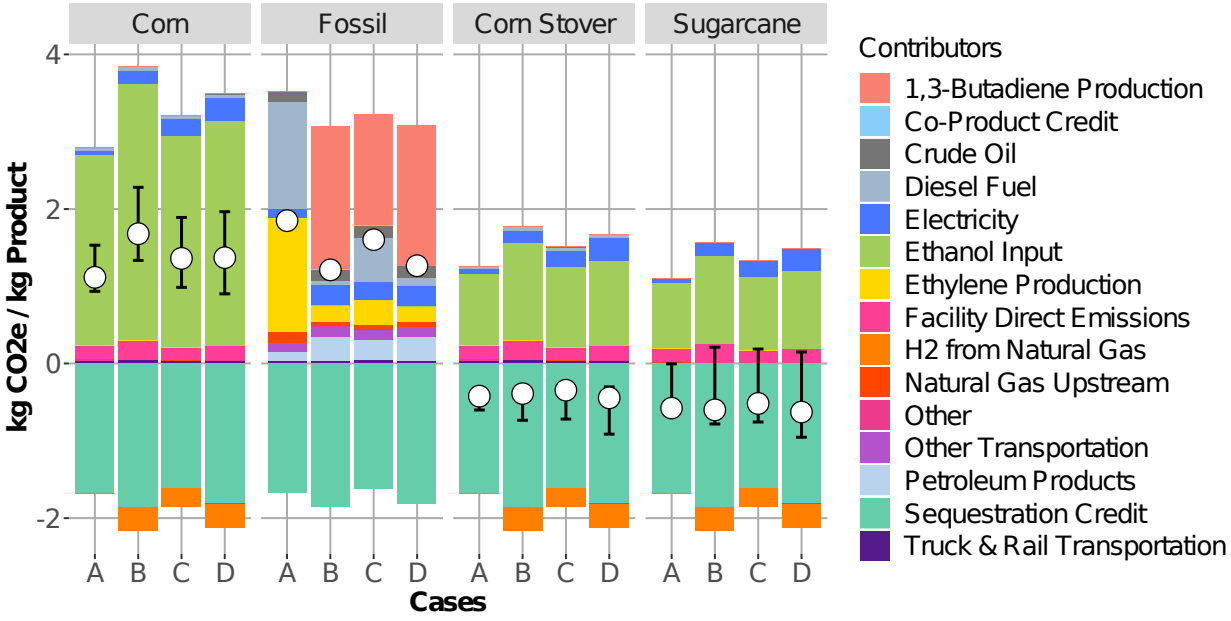

Figure 6: Life-Cycle Greenhouse Gas Emissions for Each Production Pathway

Our results indicate that the feedstock used to produce the ethanol input is an important driver of GHG emissions. Corn stover- and sugarcane-derived ethanol routes both achieve substantial reductions in emissions relative to the conventional fossil routes, whereas use of corn grain ethanol results in either very small reductions or small increases in net emissions if indirect land use change (iLUC) and any direct land use change emissions (net loss of soil carbon, for example) are not included (see Figure 7). Sensitivity bars capture variations in the local electricity mix, distance ethanol is shipped from the point of origin to the conversion facility, and variations in the carbon-intensity of ethanol production due to fuel choices at the biorefinery and feedstock cultivation/harvesting practices. Numeric versions of the average case results are presented in Table S5.

Table 3 shows the reductions in GHG emissions relative to the conventional fossil route for the combinations of each Case and ethanol feedstock, in terms of percentage reduction, total reduction per kg of product mix, and reductions per kg of ethanol input. Only Case A (which produces mostly ethylene) results in an appreciable GHG reduction of 40% if corn grain ethanol is used. Biorefineries using corn stover or sugarcane-derived ethanol, achieve dramatic GHG emissions reductions, reaching as high as 150%. Cases B and D, using sugarcane-derived ethanol, achieve the largest relative reductions in emissions (approximately 150%). This is because the footprint of those conventional fossil routes are lower, and these numbers serve as the denominator in the fractional GHG reduction. Cases A and C achieve 120-130% reductions if corn stover or sugarcane ethanol are used. Regardless of ethanol source, Case A achieves the greatest absolute reduction in emissions per kg of product mix or kg of ethanol input relative to the fossil route because the conventional fossil route is most carbon-intensive (and the mass product yield per kg of ethanol is also highest in Case A, as shown in Figure 4).

Table 3: Greenhouse Gas Emissions Reductions by Case and Ethanol Feedstock

Feedstock	Case	Net kg CO2e / kg product	Percent reduction relative to fossil	Total reduction (kg CO2e / kg product)	Total reduction (kg CO2e / kg ethanol input)
Corn	A	1.12	40%	0.73	0.49
Stover	A	-0.42	123%	2.27	1.51
Sugarcane	A	-0.58	131%	2.43	1.61
Fossil	A	1.85	N/A	N/A	N/A
Corn	B	1.68	-39%	-0.47	-0.23
Stover	B	-0.39	132%	1.60	0.79
Sugarcane	B	-0.60	149%	1.81	0.90
Fossil	B	1.21	N/A	N/A	N/A
Corn	C	1.36	15%	0.24	0.15

Stover	C	-0.34	122%	1.95	0.96
Sugarcane	C	-0.52	132%	2.12	1.05
Fossil	C	1.60	N/A	N/A	N/A
Corn	D	1.37	-8%	-0.11	-0.06
Stover	D	-0.44	135%	1.71	0.96
Sugarcane	D	-0.63	150%	1.89	1.07
Fossil	D	1.27	N/A	N/A	N/A

Discussion

Production of bio-based chemicals is considered a vital part of any strategy for reducing crude oil consumption, and the products explored here have the potential to penetrate particularly high-volume markets [1]. We have presented a set of strategies for producing varying combinations of platform chemicals for rubber (1,3-BD) and plastic (ethylene) production, as well as a diesel fuel replacement (DEE). Starting from bio-ethanol we were able to produce 1,3-butadiene in selectivity up to 60% in one-step reaction. The key to success was the introduction of ZnO as redox site on the Ta_2O_5-SiO_2. By doing so, ethanol could be dehydrogenated in-situ to produce acetaldehyde which is a crucial intermediate for this transformation. In addition, our catalysts also showed long-term stability, with TOS > 120 h reported. By varying the catalyst components, we were able to tune the acidity and basicity of the catalysts, which allowed us to selectively produce different product distributions. This flexibility can be valuable in unstable market conditions, if facilities can be quickly transitioned to using a different catalyst to maximize the highest-value outputs. That said, downstream separations will pose a challenge, and this may limit the degree to which facilities can vary their product mix without significant, expensive retrofits. Future work will be focused on finely tuning and optimizing the catalyst components to improve the conversion of ethanol and selectivity to targeted products and reduce the required reactor sizes. Additional future work is needed to better understand the degree to which product fractions can be varied without requiring changes in capital equipment, and the potential advantages to accepting ethanol feed streams with higher water content than what is required for anhydrous ethanol.

In the simulated scale-up of selected results, our models indicate that the four case studies explored can achieve dramatic GHG emissions reductions if sugarcane- or corn stover-derived ethanol is used as a feedstock, reaching as much as a 150% reduction in GHG-intensity relative to the conventional fossil pathways (meaning there is net sequestration of biogenic carbon compared to net emissions in the fossil case). In the case of corn grain ethanol, the GHG-intensity is similar to that of the fossil pathways for most

cases, but a 40% emission reduction can be achieved in Case A (which produces primarily ethylene and DEE). If the sole goal is to maximize emissions reductions per kg of ethanol diverted from other markets, Case A is the clear choice. It is likely, however, that Case A is not the most economically favorable route and further analysis should comprehensively compare costs with market prices. Our results highlight the value of combining empirical studies with chemical process modeling and life-cycle assessment. By simulating operations at commercial scale, we are able to identify differences in biorefinery energy needs, potential co-products that must be exported (e.g. hydrogen), and to gauge the relative benefits of different product mixes from a practical and environmental standpoint.

Acknowledgements

Preparation of this article was supported in part by the Energy Biosciences Institute at the University of California, Berkeley. This work was part of the DOE Joint BioEnergy Institute (http:// www.jbei.org) supported by the U.S. Department of Energy, Office of Science, Office of Biological and Environmental Research, through contract DE-AC02-05CH11231 between Lawrence Berkeley National Laboratory and the U.S. Department of Energy. The United States Government retains and the publisher, by accepting the article for publication, acknowledges that the United States Government retains a non-exclusive, paid-up, irrevocable, world-wide license to publish or reproduce the published form of this manuscript, or allow others to do so, for United States Government purposes.

Supporting Information: Materials, catalyst preparation, catalyst characterization, catalyst tests, life-cycle assessment assumptions and input data, life-cycle assessment numerical results

References

(1) *Replacing the Whole Barrel To Reduce U.S. Dependence on Oil*; U.S. Department of Energy: Washington, DC, 2013.

(2) González-Pajuelo, M.; Meynial-Salles, I.; Mendes, F.; Andrade, J. C.; Vasconcelos, I.; Soucaille, P. Metabolic Engineering of Clostridium Acetobutylicum for the Industrial Production of 1,3-Propanediol from Glycerol. *Metab. Eng.* **2005**, *7* (5–6), 329–336, DOI http://dx.doi.org/10.1016/j.ymben.2005.06.001.

(3) Meynial-Salles, I.; Dorotyn, S.; Soucaille, P. A New Process for the Continuous Production of Succinic Acid from Glucose at High Yield, Titer, and Productivity. *Biotechnol. Bioeng.* **2008**, *99* (1), 129–135, DOI 10.1002/bit.21521.

(4) Raynaud, C.; Sarçabal, P.; Meynial-Salles, I.; Croux, C.; Soucaille, P. Molecular Characterization of the 1,3-Propanediol (1,3-PD) Operon of

Clostridium Butyricum. *Proc. Natl. Acad. Sci.* **2003**, *100* (9), 5010–5015, DOI 10.1073/pnas.0734105100.
(5) Angelici, C.; Weckhuysen, B. M.; Bruijnincx, P. C. A. Chemocatalytic Conversion of Ethanol into Butadiene and Other Bulk Chemicals. *ChemSusChem* **2013**, *6* (9), 1595–1614, DOI 10.1002/cssc.201300214.
(6) Scown, C. D.; Taptich, M.; Horvath, A.; McKone, T. E.; Nazaroff, W. W. Achieving Deep Cuts in the Carbon Intensity of U.S. Automobile Transportation by 2050: Complementary Roles for Electricity and Biofuels. **2013**, *47* (16), 9044–9052, DOI 10.1021/es4015635.
(7) Foo, J. L.; Jensen, H. M.; Dahl, R. H. Improving Microbial Biogasoline Production in Escherichia Coli Using. *MBio* **2014**, *5* (6), 1–9, DOI 10.1128/mBio.01932-14.Invited.
(8) Frederix, M.; Mingardon, F.; Hu, M.; Sun, N.; Pray, T.; Singh, S.; Simmons, B. A.; Keasling, J. D.; Mukhopadhyay, A. Development of an: E. Coli Strain for One-Pot Biofuel Production from Ionic Liquid Pretreated Cellulose and Switchgrass. *Green Chem.* **2016**, *18* (15), 4189–4197, DOI 10.1039/c6gc00642f.
(9) Humbird, D.; Davis, R.; Tao, L.; Kinchin, C.; Hsu, D.; Aden, A.; Schoen, P.; Lukas, J.; Olthof, B.; Worley, M.; et al. *Process Design and Economics for Biochemical Conversion of Lignocellulosic Biomass to Ethanol*; National Renewable Energy Laboratory: Golden, CO, 2011.
(10) Posada, J. A.; Patel, A. D.; Roes, A.; Blok, K.; Faaij, A. P. C.; Patel, M. K. Potential of Bioethanol as a Chemical Building Block for Biorefineries: Preliminary Sustainability Assessment of 12 Bioethanol-Based Products. *Bioresour. Technol.* **2013**, *135*, 490–499, DOI 10.1016/j.biortech.2012.09.058.
(11) Bailey, B.; Eberhardt, J.; Goguen, S.; Erwin, J. *Diethyl Ether (DEE) as a Renewable Diesel Fuel*; SAE technical paper, 1997.
(12) Cespi, D.; Passarini, F.; Vassura, I.; Cavani, F. Butadiene from Biomass, a Life Cycle Perspective to Address Sustainability in the Chemical Industry. *Green Chem.* **2016**, *18* (6), 1625–1638, DOI 10.1039/C5GC02148K.
(13) Shylesh, S.; Gokhale, A. A.; Scown, C. D.; Kim, D.; Ho, C. R.; Bell, A. T. From Sugars to Wheels: The Conversion of Ethanol to 1,3-Butadiene over Metal-Promoted Magnesia-Silicate Catalysts. *ChemSusChem* **2016**, *9* (12), 1462–1472, DOI 10.1002/cssc.201600195.
(14) Pomalaza, G.; Capron, M.; Ordomsky, V.; Dumeignil, F. Recent Breakthroughs in the Conversion of Ethanol to Butadiene. *Catalysts* **2016**, *6* (12), 203, DOI 10.3390/catal6120203.
(15) Makshina, E. V; Janssens, W.; Sels, B. F.; Jacobs, P. A. Catalytic Study of the Conversion of Ethanol into 1,3-Butadiene. *Catal. Today* **2012**, *198* (1), 338–344, DOI http://dx.doi.org/10.1016/j.cattod.2012.05.031.
(16) Baylon, R. A. L.; Sun, J.; Wang, Y. Conversion of Ethanol to 1,3-Butadiene over Na Doped ZnxZryOz Mixed Metal Oxides. *Catal. Today* **2016**, 446–452, DOI 10.1016/j.cattod.2015.04.010.
(17) Niiyama, H.; Morii, S.; Echigoya, E. Butadiene Formation from Ethanol

over Silica-Magnesia Catalysts. *Bull. Chem. Soc. Jpn.* **1972**, *45* (3), 655–659, DOI 10.1246/bcsj.45.655.
(18) Kvisle, S.; Aguero, A.; Sneeden, R. P. A. Transformation Of Ethanol into 1,3-Butadiene Over Magnesium-Oxide Silica Catalysts. *Appl. Catal.* **1988**, *43* (1), 117–131, DOI 10.1016/S0166-9834(00)80905-7.
(19) Bhattacharyya, S. K.; Ganguly, N. D. One-Step Catalytic Conversion of Ethanol to Butadiene in the Fixed Bed. II. Binary- and Ternary-Oxide Catalysis. *J. Appl. Chem.* **1962**, *12* (3), 105–110, DOI 10.1002/jctb.5010120302.
(20) Corson, B. B.; Jones, H. E.; Welling, C. E.; Hinckley, J. A.; Stahly, E. E. Butadiene from Ethyl Alcohol. Catalysis in the One-and Two-Stop Processes. *Ind. Eng. Chem.* **1950**, *42* (2), 359–373, DOI 10.1021/ie50482a039.
(21) Kim, T.-W.; Kim, J.-W. J.-R.; Kim, S.-Y.; Chae, H.-J.; Kim, J.-W. J.-R.; Jeong, S.-Y.; Kim, C.-U. Butadiene Production from Bioethanol and Acetaldehyde over Tantalum Oxide-Supported Spherical Silica Catalysts for Circulating Fluidized Bed. *Chem. Eng. J.* **2015**, *278*, 217–223, DOI 10.1016/j.cej.2014.09.110.
(22) Chieregato, A.; Velasquez Ochoa, J.; Bandinelli, C.; Fornasari, G.; Cavani, F.; Mella, M.; Velasquez Ochoa, J.; Bandinelli, C.; Fornasari, G.; Cavani, F.; et al. On the Chemistry of Ethanol on Basic Oxides: Revising Mechanisms and Intermediates in the Lebedev and Guerbet Reactions. *ChemSusChem* **2015**, *8* (2), 377–388, DOI 10.1002/cssc.201402632.
(23) Jones, M. D. Catalytic Transformation of Ethanol into 1,3-Butadiene. *Chem. Cent. J.* **2014**, *8* (1), 53, DOI 10.1186/s13065-014-0053-4.
(24) Makshina, E. V; Dusselier, M.; Janssens, W.; Degreve, J.; Jacobs, P. A.; Sels, B. F. Review of Old Chemistry and New Catalytic Advances in the On-Purpose Synthesis of Butadiene. *Chem. Soc. Rev.* **2014**, *43* (22), 7917–7953, DOI 10.1039/C4CS00105B.
(25) Angelici, C.; Velthoen, M. E. Z.; Weckhuysen, B. M.; Bruijnincx, P. C. A. Influence of Acid–Base Properties on the Lebedev Ethanol-to-Butadiene Process Catalyzed by SiO_2–MgO Materials. *Catal. Sci. Technol.* **2015**, *5* (5), 2869–2879, DOI 10.1039/C5CY00200A.
(26) Angelici, C.; Velthoen, M. E. Z.; Weckhuysen, B. M.; Bruijnincx, P. C. A. Effect of Preparation Method and CuO Promotion in the Conversion of Ethanol into 1,3-Butadiene over SiO2–MgO Catalysts. *ChemSusChem* **2014**, *7* (9), 2505–2515, DOI 10.1002/cssc.201402361.
(27) Lewandowski, M.; Babu, G. S.; Vezzoli, M.; Jones, M. D.; Owen, R. E.; Mattia, D.; Plucinski, P.; Mikolajska, E.; Ochenduszko, A.; Apperley, D. C. Investigations into the Conversion of Ethanol to 1,3-Butadiene Using MgO:SiO2 Supported Catalysts. *Catal. Commun.* **2014**, *49*, 25–28, DOI 10.1016/j.catcom.2014.02.003.
(28) Da Ros, S.; Jones, M. D.; Mattia, D.; Pinto, J. C.; Schwaab, M.; Noronha, F. B.; Kondrat, S. A.; Clarke, T. C.; Taylor, S. H. Ethanol to 1,3-Butadiene Conversion by Using ZrZn-Containing MgO/SiO2 Systems Prepared by Co-Precipitation and Effect of Catalyst Acidity Modification.

ChemCatChem **2016**, *8* (14), 2376–2386, DOI 10.1002/cctc.201600331.
(29) Stürzel, M.; Mihan, S.; Mülhaupt, R. From Multisite Polymerization Catalysis to Sustainable Materials and All-Polyolefin Composites. *Chem. Rev.* **2016**, *116* (3), 1398–1433, DOI 10.1021/acs.chemrev.5b00310.
(30) Goulas, K. A.; Sreekumar, S.; Song, Y.; Kharidehal, P.; Gunbas, G.; Dietrich, P. J.; Johnson, G. R.; Wang, Y. C.; Grippo, A. M.; Grabow, L. C.; et al. Synergistic Effects in Bimetallic Palladium–Copper Catalysts Improve Selectivity in Oxygenate Coupling Reactions. *J. Am. Chem. Soc.* **2016**, *138* (21), 6805–6812, DOI 10.1021/jacs.6b02247.
(31) Sushkevich, V. L.; Ivanova, I. I.; Taarning, E. Ethanol Conversion into Butadiene over Zr-Containing Molecular Sieves Doped with Silver. *Green Chem.* **2015**, *17* (4), 2552–2559, DOI 10.1039/C4GC02202E.
(32) Larina, O. V; Kyriienko, P. I.; Soloviev, S. O. Ethanol Conversion to 1,3-Butadiene on ZnO/MgO–SiO2 Catalysts: Effect of ZnO Content and MgO:SiO2 Ratio. *Catal. Letters* **2015**, *145* (5), 1162–1168, DOI 10.1007/s10562-015-1509-4.
(33) De Baerdemaeker, T.; Feyen, M.; Müller, U.; Yilmaz, B.; Xiao, F.-S.; Zhang, W.; Yokoi, T.; Bao, X.; Gies, H.; De Vos, D. E. Bimetallic Zn and Hf on Silica Catalysts for the Conversion of Ethanol to 1,3-Butadiene. *ACS Catal.* **2015**, *5* (6), 3393–3397, DOI 10.1021/acscatal.5b00376.
(34) Musˇicˇ, A.; Batista, J.; Levec, J. Gas-Phase Catalytic Dehydrogenation of Methanol to Formaldehyde over ZnO/SiO2 Based Catalysts, Zeolites, and Phosphates. *Appl. Catal. A Gen.* **1997**, *165* (1), 115–131, DOI 10.1016/S0926-860X(97)00195-6.
(35) Suchorska-Woźniak, P.; Rac, O.; Klimkiewicz, R.; Fiedot, M.; Teterycz, H. Dehydrogenation Properties of ZnO and the Impact of Gold Nanoparticles on the Process. *Appl. Catal. A Gen.* **2016**, *514*, 135–145, DOI 10.1016/j.apcata.2016.01.020.
(36) *Ethylene Uses and Market Data*; International Chemical Information Service (ICIS), 2007.
(37) Christensen, C. H.; Rass-Hansen, J.; Marsden, C. C.; Taarning, E.; Egeblad, K. The Renewable Chemicals Industry. *ChemSusChem* **2008**, *1* (4), 283–289, DOI 10.1002/cssc.200700168.
(38) Janssens, W.; Makshina, E. V; Vanelderen, P.; De Clippel, F.; Houthoofd, K.; Kerkhofs, S.; Martens, J. A.; Jacobs, P. A.; Sels, B. F. Ternary Ag/MgO-SiO 2 Catalysts for the Conversion of Ethanol into Butadiene. *ChemSusChem* **2015**, *8* (6), 994–1008, DOI 10.1002/cssc.201402894.
(39) White, W. C. Butadiene Production Process Overview. *Chem. Biol. Interact.* **2007**, *166* (1–3), 10–14, DOI 10.1016/j.cbi.2007.01.009.
(40) *Chemical Economics Handbook: Ethyl Ether*; IHS, Inc.: London, U.K., 2014.
(41) Senthil, R.; Sivakumar, E.; Silambarasan, R. Effect of Di Ethyl Ether on the Performance and Emission Characteristics of a Diesel Engine Using Biodiesel-Eucalyptus Oil Blends. *RSC Adv.* **2015**, *5* (67), 54019–54027, DOI 10.1039/c5ra08414h.
(42) Duncan Seddon. *Butadiene Price History and Trends (Sept 2012)*; 2012.

(43) Hodges, P. *Butadiene Price Collapse Sends Warning on H2 Demand*; International Chemical Information Service (ICIS), 2013.
(44) Posada, J. A.; Patel, A. D.; Roes, A.; Blok, K.; Faaij, A. P. C.; Patel, M. K. Potential of Bioethanol as a Chemical Building Block for Biorefineries: Preliminary Sustainability Assessment of 12 Bioethanol-Based Products. *Bioresour. Technol.* **2013**, *135*, 490–499.
(45) Scown, C. D. C. D.; Gokhale, A. A. A. A.; Willems, P. A. P. A.; Horvath, A.; McKone, T. E. T. E. Role of Lignin in Reducing Life-Cycle Carbon Emissions, Water Use, and Cost for United States Cellulosic Biofuels. **2014**, *48* (15), 8446–8455, DOI 10.1021/es5012753.
(46) Balakrishnan, M.; Sacia, E. R. E. R.; Sreekumar, S.; Gunbas, G.; Gokhale, A. A. A. A.; Scown, C. D. C. D.; Toste, F. D. D.; Bell, A. T. A. T. Novel Pathways for Fuels and Lubricants from Biomass Optimized Using Life-Cycle Greenhouse Gas Assessment. **2015**, *112* (25), 7645–7649, DOI 10.1073/pnas.1508274112.
(47) Neupane, B.; Konda, N. V. S. N. M.; Singh, S.; Simmons, B. A.; Scown, C. D. Life-Cycle Greenhouse Gas and Water Intensity of Cellulosic Biofuel Production Using Cholinium Lysinate Ionic Liquid Pretreatment. *ACS Sustain. Chem. Eng.* **2017**, *5* (11), DOI 10.1021/acssuschemeng.7b02116.
(48) Knaeble, W.; Iglesia, E. Kinetic and Theoretical Insights into the Mechanism of Alkanol Dehydration on Solid Brønsted Acid Catalysts. *J. Phys. Chem. C* **2016**, *120* (6), 3371–3389, DOI 10.1021/acs.jpcc.5b11127.
(49) Davis, R.; Tao, L.; Scarlata, C.; Tan, E. C. D.; Ross, J.; Lukas, J.; Sexton, D. *Process Design and Economics for the Conversion of Lignocellulosic Biomass to Hydrocarbons: Dilute-Acid and Enzymatic Deconstruction of Biomass to Sugars and Catalytic Conversion of Sugars to Hydrocarbons*; National Renewable Energy Laboratory: Golden, CO, 2015.
(50) Weidema, B. Avoiding Co-Product Allocation in Life-Cycle Assessment. *J. Ind. Ecol.* **2001**, *4* (3), 11–33, DOI 10.1162/108819800300106366.
(51) Wang, M.; Lee, H.; Molburg, J. Allocation of Energy Use in Petroleum Refineries to Petroleum Products. *Int. J. Life Cycle Assess.* **2004**, *9* (1), 34–44, DOI 10.1007/BF02978534.
(52) Ozalp, N.; Hyman, B. Allocation of Energy Inputs Among the End-Uses in the U.S. Petroleum and Coal Products Industry. *Energy* **2007**, *32*, 1460–1470, DOI 10.1016/j.energy.2006.09.006.
(53) Guinée, J.; Heijungs, R.; Huppes, G. Economic Allocaton: Examples and Derived Decision Tree. *Int. J. Life Cycle Assess.* **2004**, *9* (1), 23–33, DOI 10.1007/BF02978533.
(54) Themelis, N. J.; Mussche, C. *2014 Energy and Economic Value of Municipal Solid Waste (MSW) and Non-Recycled Plastics (NRP) Currently Landfilled in the Fifty States*; Columbia University Earth Engineering Center: New York, NY, 2014.
(55) Keoleian, G.; Miller, S.; Kleine, R. D.; Fang, A.; Mosley, J. Life Cycle Material Data Update for GREET Model. *Rep. No. CSS12-12* **2012**.

For Table of Contents Use Only

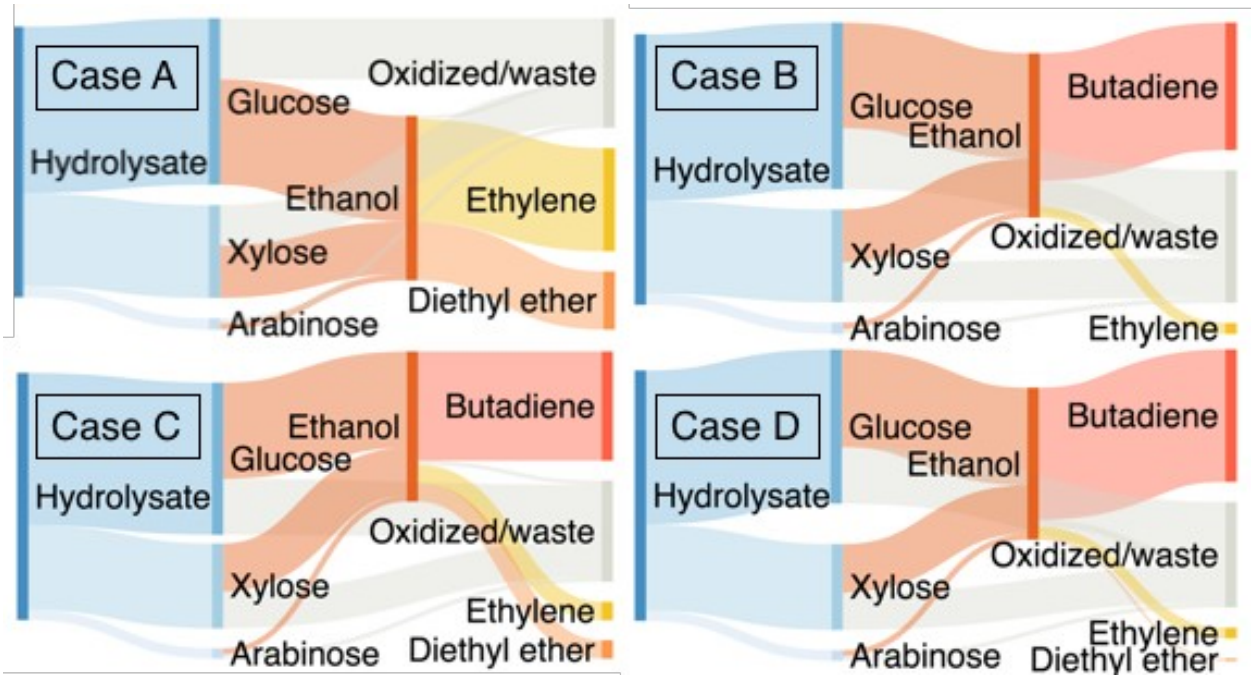

Synopsis:

Tuning the catalyst and reaction conditions changes the flow of carbon from the feedstock to the suite of fuel and chemical products.